Kinetics of Specific and Nonspecific Adhesion of Red Blood Cells on Glass

Z. Xia,*‡ H. L. Goldsmith,§ and T. G. M. van de Ven*‡
*Paprican and Departments of ‡Chemistry and §Medicine, Pulp and Paper Research Centre, McGill University, Montreal, H3A 2A7 Canada

ABSTRACT Fixed spherical human red blood cells suspended in 17% sucrose were allowed to adhere on either clean glass surfaces or glass surfaces preincubated with antibodies specific to a certain blood group antigen. The adhesion experiments were performed in an impinging jet apparatus, in which the cells are subjected to stagnation point flow. The objective of this study was to compare the efficiencies of nonspecific and specific (antigen-antibody mediated) adhesion of red blood cells on glass surfaces. The efficiency was defined as the ratio of the experimental adhesion rate to that calculated based on numerical solutions of the mass transfer equation, taking into account hydrodynamic interactions as well as colloidal forces. The efficiency for nonspecific adhesion was nearly unity at flow rates lower than 85 μl/s (corresponding to a wall shear rate, G_w, of 30 s^{-1} at a radial distance of 110 μm from the stagnation point). The values of efficiency dropped at higher flow rates, due to an increase in the tangential force. The critical deposition concentration is found to occur at 120–150 mM NaCl, which is consistent with the theoretically predicted values. At low salt concentrations, the experimental values are higher than the theoretical ones. Similar discrepancies have been found in many colloidal systems. Introducing steric repulsion by adsorbing a layer of albumin molecules on the glass completely prevents nonspecific adhesion at flow rates below 60 μl/s ($G_w \simeq 15$ s^{-1}). The efficiency of specific adhesion depends both on the concentration of antibody molecules on the surface and the flow rate. Normal red cells adhere more readily through antigen-antibody bonds than fixed cells. Fixed spherical cells have a higher adhesion efficiency than fixed biconcave ones.

INTRODUCTION

Cell adhesion can be regulated by nonspecific forces, such as van der Waals attraction and electrostatic repulsion, which govern the interactions between all colloidal particles and substrates, as well as by specific affinities between adhesive molecules (ligands and receptors) on cells and substrate or between cells in the suspending medium. Examples of the latter are antigen-antibody reactions. The expression of the specific affinity is, in turn, usually regulated by some biological event, such as conformational change, clustering, and dimerization of the adhesive molecules, as well as morphological changes of the cells. Red blood cells have been the preferred models for both nonspecific and specific cell-substrate adhesion, due to their simpler structure, their lack of cytoskeletal activity, their morphological changes in response to various chemical and physical stimuli, and their well understood chemical, mechanical (Evans, 1983; Evans and Kukan, 1983; Vertessy and Steck 1989), rheological (Goldsmith and Marlow, 1979; Dintenfass, 1990), and colloidal properties (Donath and Voight, 1986; Crunze and Heuck, 1986). Adhesion studies of red blood cells have been conducted on various materials, including glass (Wolf and Gingell, 1983; Trommler et al., 1985) and polymer surfaces (Absolom et al., 1986), as well as oil/water interfaces (Gingell and Todd, 1975). The emphasis has usually been placed on the influence of physicochemical factors, such as ionic strength, pH, temperature, and osmolarity. Such work has been motivated by problems of biocompatibility or the desire to understand the mechanism of adhesion.

Cells, however, are normally exposed to body fluids which not only serve as mechanical stimulators (i.e., causing extension, compression, and shear of cell membranes), but also control the dynamic process of adhesion. The flow of body fluids may, for example, bring cells and substrates into contact by overcoming possible repulsive barriers due to steric or electrostatic repulsion, or, contrarily, remove a cell from another cell or substrate before a "key" molecule finds its way into the specific cavity of a "lock" molecule. Therefore, studies on static adhesion of red cells based on pre-exposure of cells to a substrate, followed by detachment of nonadherent cells by external forces, such as gravity (Weiss, 1974), centrifugation (Trommler et al., 1985), or hydrodynamic shear (Shiga et al., 1985) are inadequate to reflect the in vivo situation. Besides thermodynamics, the kinetic aspects must also be considered. For this reason, more attention has recently been directed to the time dependence of the adhesion process. The technique most commonly adopted to study the time dependence is one in which a number of parallel static adhesion batch experiments is performed, terminated, and analyzed successively (Volger and Bussian, 1987). Another method consists of passing cells through a column packed with beads made of the particular material of interest and detecting the variation in particle concentration of the effluent with time (Kallay and Matijevic, 1981). A variety of flow chambers, such as the parallel plate channel (Chien et al., 1990), the rotating disk (Hull and Kitchener, 1969; Rutter and Abbott, 1978) and the radial flow chamber (Fowler and Mckay, 1980) have been developed to better control the hydrodynamic forces. Most of these techniques, however, serve

Received for publication 14 January 1993 and in final form 14 May 1993.
Address reprint requests to T. G. M. van de Ven.

0006-3495/93/09/1073/11 $2.00

to measure the kinetics of detachment, i.e., to characterize the duration of adhesive bonds with respect to hydrodynamic forces and time. For instance, transient adhesion of model cells in an axisymmetric stagnation point flow created by a radial flow chamber was studied (Cozens-Roberts et al., 1990) by monitoring the critical radii beyond which the model cells survived the shear force and remained adherent.

Our impinging jet technique, so far used to study adhesion of latex particles (Dabros and van de Ven, 1983; Varennes and van de Ven, 1988a) and bacteria (Xia et al., 1989), also creates a stagnation point flow. However, instead of focusing on areas at a large distance from the stagnation point (as was the case in the radial flow chamber technique), we are interested in the small area near the stagnation point, where the hydrodynamic boundary layer is relatively thin and uniform. Hence, the continuously measured surface density can be interpreted by theories of mass transport and colloidal interactions, considering the probability of receptor/ligand collisions.

The objective of this study is to gain a better understanding of the kinetics of both nonspecific and specific (antigen-antibody mediated) adhesion of red blood cells in terms of mass transport and hydrodynamic theories, taking into account the colloidal forces.

EXPERIMENTAL

Preparation of fixed sphered swollen red blood cells

Fixed spherical red blood cells (FSRC) were prepared by the method of Tha et al. (1986). Essentially, blood obtained from healthy volunteers via venipuncture into EDTA coated test tubes was centrifuged at 80 g to separate the red blood cells from plasma. The buffy coat was removed by aspiration of the supernatant during the repeated washing (six times) in ice-cold isotonic phosphate buffer (PB) containing 1 mM Mg^{2+} (pH 7.4). 1 ml of packed biconcave red cells was allowed to swell to spheres in 104-ml hypotonic PB solution containing 0.2 M glycerol and 1.73 mM SDS. After about 15 s of stirring, they were fixed by freshly prepared 1% electron microscope grade glutaraldehyde (Fisher Scientific, Montreal, Que.) solution in PB at a final concentration of 0.085%. The fixed spherical red cells were washed six times in a physiological saline (PS) solution, 0.15 M NaCl in distilled deionized water, and were stored in saline containing 0.01% sodium azide at 4°C for a maximum period of 2 weeks before use.

The average diameter of the FSRC so prepared was 6.1 ± 0.4 μm determined from diffusion coefficient measurement by photon correlation spectroscopy (PCS). The differences between three different batches (from two different donors) were within 8% by PCS measurements. This size is in good agreement with microscopic observations under a magnification of 800 (Zeiss Ultraphot II).

Fixed biconcave cells were also prepared by glutaraldehyde fixation as follows. To 5-ml washed red cells, 250 μl of platelet-poor plasma at 37°C was added. This suspension was mixed with 25 ml of isotonic PB containing 0.3% electron microscope grade glutaraldehyde for 5 min while being stirred. The fixed cells were washed five times in PS.

Prior to an experiment, the FSRC were suspended in a saline solution containing 17% (w/w) sucrose (pH 6.5–6.8) to avoid sedimentation during the experimental period, typically 30 min. The concentrations of the red cell suspensions were determined, by counting the number of cells in a hemacytometer, and then adjusted to the desired values.

Estimation of FSRC density

Dilute suspensions of red cells in distilled deionized water (120 cells μl^{-1}, corresponding to a volume fraction of 0.001%) were titrated with 30% sucrose solution while being mixed by a magnetic stirrer. The resulting suspensions were then allowed to stand for 1–2 h. The sucrose concentration was calculated when no obvious phase separation was observed. The density (1.08 kg dm^{-3}) of the sucrose solution (19.9% by weight) was taken as the density of the fixed red blood cells.

Adsorption of antibody on glass surfaces

Glass coverslips (Fisher Scientific, Pittsburgh, PA), cleaned using a previously described procedure (Xia et al., 1989), were incubated overnight with monoclonal mouse antihuman IgM antibody (Dako Corporation, Dimension Labs., Mississauga, Ontario) specific to the human blood group antigen (type B) in 0.15 M NaCl at 4°C. The coated coverslips were separated from the coating solutions and incubated in saline containing 1% bovine serum albumin (BSA) for 2 h. Before experiments, a coated slip was rinsed three times with 1% BSA/saline solution.

The existence of the adsorbed antibody on glass surfaces was tested qualitatively with alkaline phosphatase conjugate of anti-mouse Ig molecules. Briefly, the coverslips, which were coated with IgM molecules and BSA successively, were incubated with phosphatase-Gα mouse Ig (Sigma Chemical Co., St. Louis, MO) at 1:350 dilution in PBS at 37°C for 2 h, followed by washing with PBS three times. They were then incubated with *p*-nitrophenyl phosphate, which scintillates after reacting with the phosphatase on the surface, in carbonate buffer (0.013 M Na_2CO_3, 0.037 M $NaHCO_3$, and 0.002 M $MgCl_2$) at the same temperature for 20 min. The optical density of the supernatant, containing *p*-nitrophenyl phosphate, at 410 nm was plotted against antibody concentration of the coating solution. The results are shown in Fig. 1. The decay in the transmittance of the supernatant, with increasing antibody concentration, indicated by the circles in the figure, demonstrates that, even after exposure to a high concentration of albumin molecules and to repeated washing, antibody molecules remain adsorbed. The squares in the figure represent the coverslips coated with antibody in the presence of 1% BSA in PBS. Obviously, albumin molecules, having a larger diffusion coefficient than antibody molecules, reach surfaces much faster than the antibody molecules and, therefore, many more albumin molecules occupy the surface.

Antibody density on glass surface

The antibody density on glass was quantified by a radioimmunoassay. The coated glass coverslips for various antibody concentrations were exposed overnight, at room temperature, to saline solutions containing known concentrations of I^{125}-labeled rat monoclonal antibody (ICN Biomedicals, Irvine, CA) against mouse IgM (Zymed Laboratories Inc., San Francisco, CA). The unbound I^{125}-labeled antibody molecules were removed by rinsing the slips 10 times with saline. The surface density of I^{125}-labeled antibody, and consequently that of the original IgM molecules, was calculated from the radioactivity of each slip determined in an x-ray spectrometer (Canberra Packard Canada Ltd., Mississauga, Ontario) assuming each and every anti-B IgM Molecule on the surface binds to one radioactive antibody molecule. The actual surface concentration of antibody could be somewhat lower than the value obtained from this method, since an IgM molecule may bind to more than one anti-IgM molecule.

Fig. 2 shows a plot of the amount of adsorbed antibody molecules and the surface coverage versus the amount of antibody molecules added. The surface coverage was calculated assuming that the diameter of an IgM molecule is 30 nm (Feinstein and Munn, 1969). It can be seen that the maximum surface coverage is rather low (only about 5%). This could be due to the presence of albumin molecules whose concentration was 1% in the original antibody solution in order to maintain the function of the antibody. These BSA molecules, whose concentration was in proportion to the antibody concentration, competed with the antibody during adsorption. For a given concentration of the coating liquid, the surface density of antibody increases approximately exponentially with time, reaching a plateau at a characteristic time which corresponds to the time required for BSA molecules to cover the surface. At a higher concentration of the coating liquid, the numbers of both BSA and IgM are increased, resulting in a shorter characteristic time and a higher plateau value. Hence, the number of antibody molecules on the

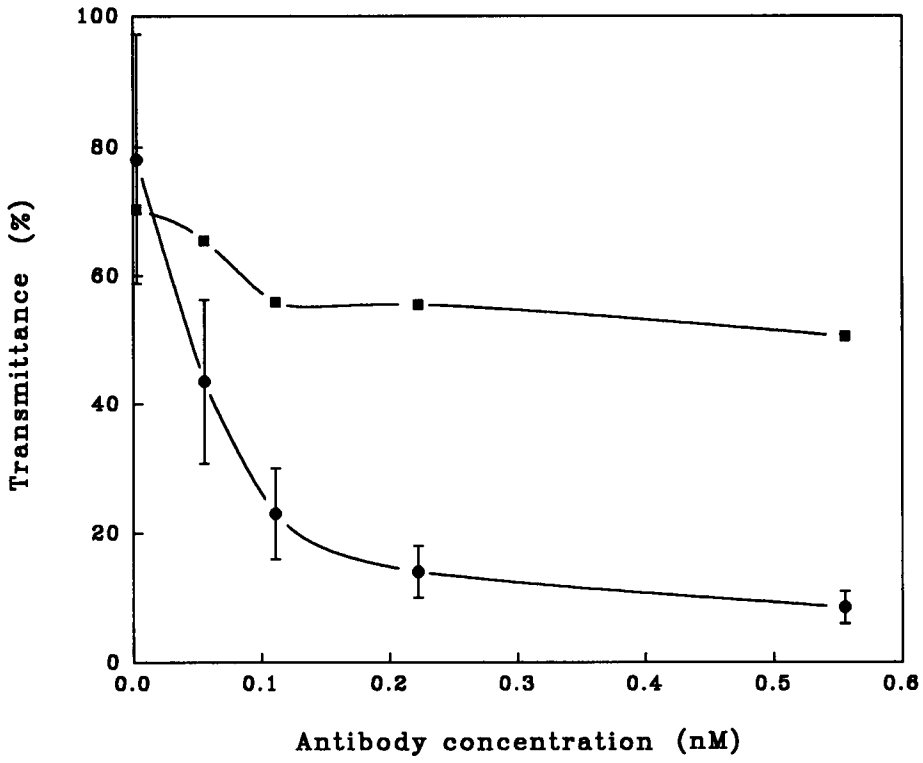

FIGURE 1 Transmittance of substrate supernatant as a function of IgM coating concentration. Circles represent the coverslips incubated with antibody prior to exposure to 1% BSA solution. Squares represent the coverslips exposed to antibody in the presence of BSA molecules.

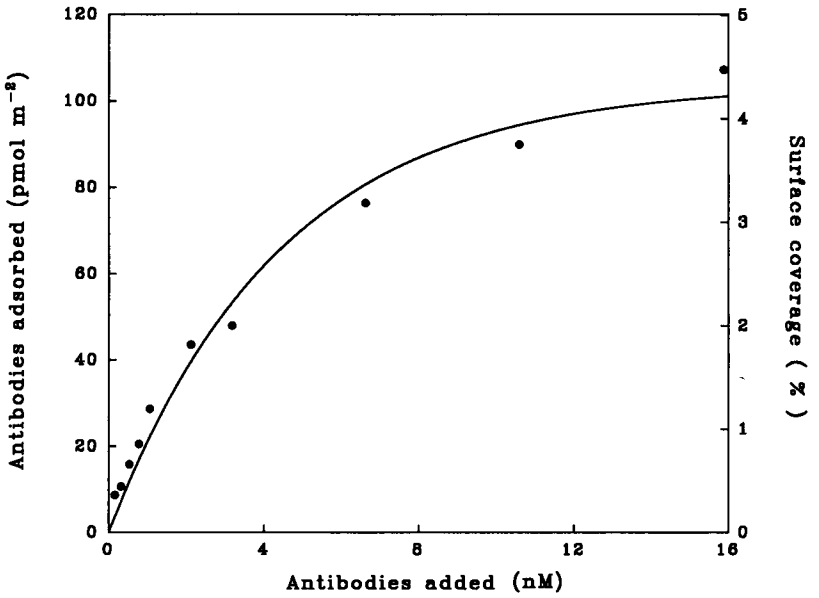

FIGURE 2 Adsorbed antibody and surface coverage as a function of IgM coating concentration. The diameter of an IgM molecule is taken as 30 nm.

surface, as shown in Fig. 2, is kinetically controlled. Since the desorption of antibody is a very slow process, equilibrium conditions will be reached after a time much longer than the duration of the experiments.

Experimental set-up

The adhesion experiments were carried out with an impinging jet apparatus, as previously described (Xia et al., 1989), and illustrated in Fig. 3. A stream of suspension (jet) flows through an orifice and impinges onto a coverslip (surface) placed on top of the flow cell. The suspension flows from a reservoir into the orifice via inlet valves by means of pressure from a nitrogen gas cylinder with a low pressure regulator which allows fine adjustment in the range of 40–140 kPa. The suspension leaves the cell via an outlet valve. For a typical flow rate of 100 μl s^{-1}, the pressure on the suspension in the gas-tight container leading to the inlet of the jet is 70 kPa. The change of flow rate due to the drop in the liquid level in the reservoir after a 30-min experiment is negligible (<1%).

The geometry of the stagnation point flow created by the impinging jet is shown in Fig. 3 *a*. The ratio of h/R of the jet was 1.8, where h is the distance between the confining plates of the jet and R is the radius of the jet. The velocity field near the stagnation point is given by

$$V_r = \alpha_s rz; \qquad V_z = -\alpha z^2 \tag{1}$$

where V_r and V_z are the velocity components in the radial (r) and normal

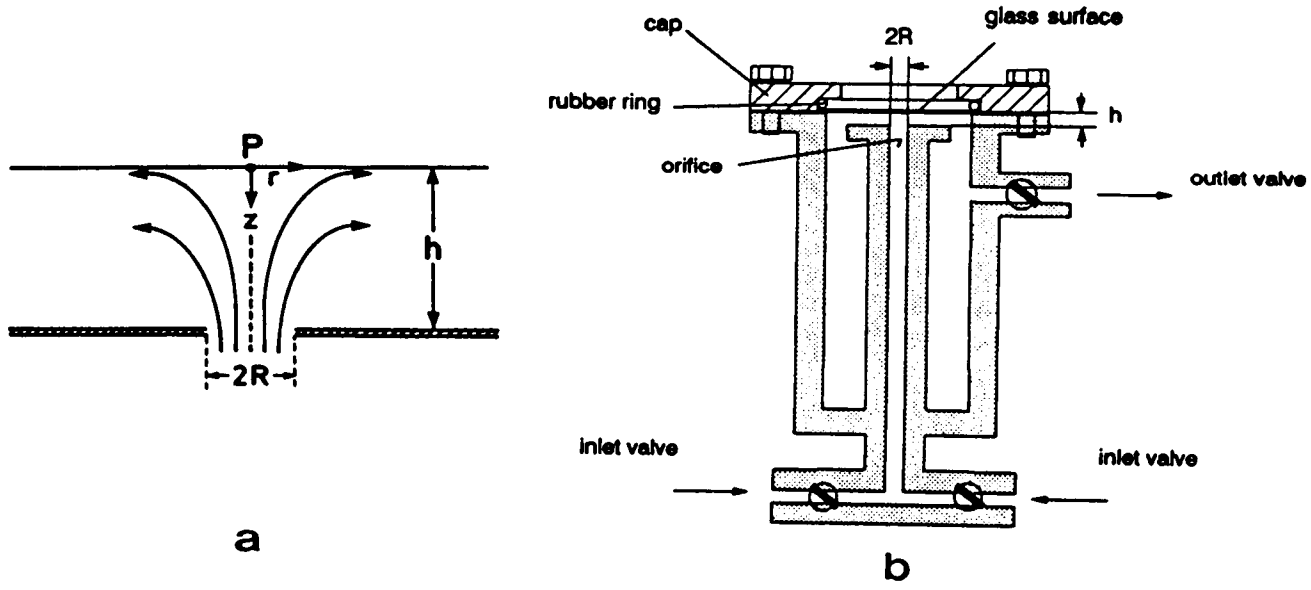

FIGURE 3 (*a*) Geometry of stagnation point flow created by a jet of radius R impinging onto a surface. After exiting from an orifice, the jet is contained between two confining plates a distance h apart. Close to the stagnation point P the flow is given by Eq. 1. (*b*) Schematic of the experimental flow cell. A suspension enters from a pressurized reservoir through an inlet valve and the orifice tube to impinge against the upper surface.

(z) direction. The parameter α_s characterizes the strength of the flow. From extrapolation of literature values (21), it can be shown that α_s is approximately given by

$$\tilde{\alpha}_s = \frac{\alpha_s R^3}{Re\nu} = 4.4Re^{1/2} - 8.24 \tag{2}$$

where ν is the kinematic viscosity of the medium and Re is the Reynolds number, defined as

$$Re = \frac{\bar{u}R\rho}{\eta} \tag{3}$$

$\bar{u}$ is the mean velocity of the jet and ρ and η are the density and the viscosity of the medium. The velocity $\bar{u}$ is determined experimentally from the amount of fluid flowing through the cell per unit time.

The number of adherent red cells on a window area of the coverslip of radius 220 μm (around the stagnation point) was observed through a microscope to which a camera was attached and recorded on video. A typical adhesion experiment lasted 20 min. The surface density, defined as the number of cells per unit area, was obtained as a function of time through frame-by-frame analysis of the videotape. From the initial linear increase of the coating density with time, the rate of adhesion was determined.

Test of the activity of antibody on the glass surface

It is possible that antibody molecules adsorbed on glass become denatured. In order to test whether antibody adsorbed on the glass surface remained active in a sucrose solution and in a flow field, fixed red blood cells suspended in 17% sucrose/saline solution at a concentration of 1.34×10^4 μl^{-1} (corresponding to a volume fraction of 0.16%) were allowed to adhere to a coated coverslip at a flow rate of 39 μl/s. Red blood cells of blood type A were used as a control to estimate the percentage of concurrent nonspecific adhesion. The results (Fig. 4) indicate that adsorbed antibody molecules maintain their function and specificity. At higher flow rates, beyond 60 μl s^{-1} a small number of A cells adhere, possibly due to detachment or rearrangement of albumin molecules on the surface under the influence of flow, thus forming bare patches on the glass surface.

THEORETICAL

For a dilute suspension, mass transfer in the absence of a source term can be expressed as

$$\frac{\partial n}{\partial t} + \nabla \cdot \mathbf{J} = 0 \tag{4}$$

$$\mathbf{J} = -\mathbf{D} \cdot \nabla n + \mathbf{U}n \tag{5}$$

where n is the concentration of the particles, $\mathbf{J}$ the particle flux vector consisting of contributions from convection and diffusion, $\mathbf{D}$ the diffusion tensor, and $\mathbf{U}$ the velocity of the particles. The velocity is the sum of the hydrodynamic velocity, obtained from Eq. 1 by multiplying the velocity components by the appropriate particle-wall correction factors, and the velocity due to forces such as colloidal and external forces. Since the adherent cells were measured in an area near the stagnation point within which the normal velocity (cf. Eq. 1) was independent of the radial distance r, the normal flux was also independent of r.

From the solution of this equation one can obtain the concentration profile of particles near the surface, from which the rate of particle deposition, j, can be calculated (Dabros and van de Ven, 1983). Usually j is expressed as a dimensionless Sherwood number defined as

$$Sh = j\frac{a}{Dn_o}, \tag{6}$$

with D being the translational diffusion constant of the particle, a its radius, and n_o the concentration. The solution of Eqs. 4 and 5 depends on the nature of the external and colloidal forces and on the ratio of convection to diffusion,

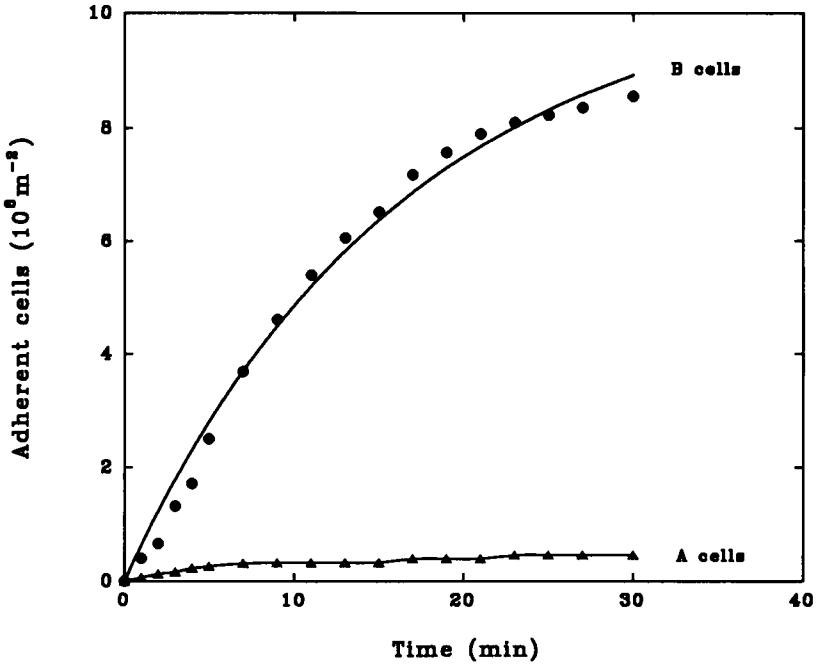

FIGURE 4 Test of the immunological activity of IgM molecules on a glass surface: surface densities of adherent fixed A cells and B cells on anti-B IgM-coated glass as a function of time. Concentration of cell suspension: 1.34×10^4 μl^{-1}; suspending medium: 17% sucrose (by weight) in saline (0.15 M NaCl); flow rate: 39 $\mu l/s$ for B cells and 37 $\mu l/s$ for A cells.

expressed by the Peclet number *Pe*:

$$Pe = \frac{2\alpha_s a^3}{D}. \tag{7}$$

For the external and colloidal forces we consider van der Waals attraction, electrostatic repulsion, and gravity. These forces are characterized by five dimensionless numbers defined as the adhesion number, $Ad = A_{123}/6kT$, the dimensionless retardation wavelength, $\lambda = \lambda/a$, the double layer number $Dl = 4\pi\epsilon\psi_1\psi_2 a/kT$, the double layer thickness parameter $\tau = \kappa a$, and the gravity number $Gr = 2\Delta\rho g a^3/9\eta D$. Here A_{123} is the Hamaker constant for dispersion interactions between surfaces 1 and 2 in medium 3, λ is the London retardation wavelength, ϵ is the permittivity of the medium, ψ_1 and ψ_2 are the surface potentials of materials 1 and 2, κ^{-1} is the double layer thickness, $\Delta\rho$ is the apparent density of the particle, g the gravitational constant, η the viscosity of the medium, and kT is the thermal energy.

Equations 4 and 5 can be solved analytically for some limiting cases; for instance, when the increase in hydrodynamic drag on a particle while approaching the surface is balanced by the van der Waals attractive force (Smoluchowski-Levich approximation) and when the diffusion boundary thickness is much greater than the particle size, i.e., the Peclet number, *Pe*, is small.

For large particles such as red blood cells, however, hydrodynamic interactions are no longer negligible, especially when *Pe* is much larger than one, typically > 200. Therefore, a numerical solution of Eqs. 4 and 5 which includes effects of both colloidal forces and hydrodynamic interactions is necessary. The boundary conditions for Eqs. 4 and 5 are

$$z/a = 1 + \delta, \quad n = 0; \qquad z \to \infty, \quad n = n_0 \tag{8}$$

where δ is taken as 1×10^{-4} (about 3 Å for a particle of 3 μm radius).

RESULTS AND DISCUSSION

Nonspecific adhesion

Parameters used in the numerical calculation

The Hamaker constant, A_{11}, for a fixed red blood cell membrane was estimated from the value of A_{132} (9×10^{-21} J) for fixed red blood cells interacting with a hexadecane/saline interface at a low salt concentration (0.3 mM NaCl) (Parsegian and Gingell, 1980) by the following equation (Visser, 1972)

$$A_{132} = \left(\sqrt{A_{11}} - \sqrt{A_{33}}\right)\left(\sqrt{A_{22}} - \sqrt{A_{33}}\right) \tag{9}$$

where the value of A_{33} was taken as that of water (3.28×10^{-20}J) (Visser, 1972) and A_{22} for hexadecane is 5.23×10^{-20}J (Hunter, 1987).

A_{33} for a 17% sucrose solution is approximately the same as that of 19% sucrose. The values for glass (1.15×10^{-19} J) (Gregory, 1969) and 19% sucrose (1.09×10^{-19} J) were calculated from the relation of the Hamaker constant and the dispersion equation of refractive index given by (Nir and Anderson, 1976)

$$A_{ik} = \frac{27}{32}\hbar C_i C_k \frac{\omega_i \omega_k}{\omega_i + \omega_k} \tag{10}$$

where $\hbar$ is Planck's constant/2π, C_i is the dispersion coefficient and ω_i is the effective frequency. From Eq. 9, A_{132} for cell/17% sucrose/glass is estimated as 0.4×10^{-21} J. From A_{123} the adhesion number was found to be $Ad = 0.02$.

Gr was calculated to be 0.223. The ratio of the radius of the cell to the double layer thickness $\tau = 4213$. The dielectric constant of 17% sucrose was estimated to be 65.3, assuming that it varies linearly with sucrose concentration. We have also assumed that λ/a is 0.4.

The electrophoretic mobility of an erythrocyte in physiological saline was experimentally determined to be 1.2×10^{-6} $ms^{-1}V^{-1}$ (Levine, et al., 1983) and theoretically predicted to be approximately 1×10^{-6} $ms^{-1}V^{-1}$, assuming that the radii of the polyelectrolyte segments are 6 Å. This mobility value corresponds to a ζ potential of −15 mV (van Oss, 1975). A ζ potential of −18 mV has also been estimated (van Oss and Absolom, 1983).

In contrast, the ζ potential of glass at high salt concentrations is rather difficult to determine. It has been measured to be larger than −56 mV in the presence of KCl at concentrations below 5 mM (Overbeek, 1952). The value obtained by extrapolating these data to 0.15 M KCl is nearly zero; however, the exact ζ potential for the physiological salt concentration is not available.

Theoretical predictions

Despite the lack of information on the zeta potential of glass, numerical solutions of Eqs. 4 and 5 show that, in the presence of 0.15 M NaCl, the critical double layer parameter, Dl_{crit}, is around 180 (Fig. 5). Below $Dl \simeq 180$, the Sherwood number, Sh, is nearly constant. This Dl value corresponds to 12 $(mV)^2$ for the product of the ζ potentials of the glass surface and the cell membrane.

Sherwood numbers calculated from Eqs. 4 and 5 with ($Sh1$) and without ($Sh2$) external forces and the correction terms for hydrodynamic interactions, are plotted for various Peclet numbers (Fig. 6). The Sherwood number $Sh2$ (the Smoluchowski-Levich approximation) is higher than $Sh1$ for all Pe values used, suggesting that for larger particles, the Smoluchowski-Levich approximation is not very good. The effect of λ and Gr on the results is very small. Varying λ/a from 0.05 to 1.0 results in an increase in $Sh1$ of 10%, while varying Gr from 0.01 to 1.0 causes an increase in $Sh1$ of only 2%.

The theory also predicts that, at low salt concentration (<0.11 M NaCl), manifested as relatively low κa values (~3000), and below a critical value of Dl the Sherwood number or adhesion rate is negligible. Increasing κa to a critical value, corresponding to the critical deposition concentration of salt (CDC), results in a dramatic rise in Sh (Fig. 7). While this abrupt change in Sh starts at the same κa, regardless of Peclet number, the CDC is shifted slightly toward higher κa values for higher Peclet numbers.

Comparison between experimental and theoretical results

The experimental Sherwood numbers were determined from the initial rate of increase in the surface density of the adherent cells, obtained from the best fit of the recorded change in the surface density with time to an exponential equation, as described previously (Xia et al., 1989). The initial slope of the equation is taken as the initial adhesion rate. Due to blocking of newly arriving cells by the adherent cells, this rate decreases gradually and, given sufficient time, approaches zero. Occasionally, the escape of an adherent cell was observed. The ratio of the experimental Sherwood number to the theoretical one, $Sh1$, is defined to be the adhesion efficiency and is denoted as α. In Fig. 8, the experimental Sherwood number and the adhesion efficiency are plotted against Peclet number. It can been seen that, except for the values at high Pe, α falls between 0.94 − 1.01, which is in excellent agreement with theory. The decrease in efficiency at high flow rates can be explained by an increase in the effects of tangential forces which were neglected in the theory (Varennes and van de Ven, 1988b).

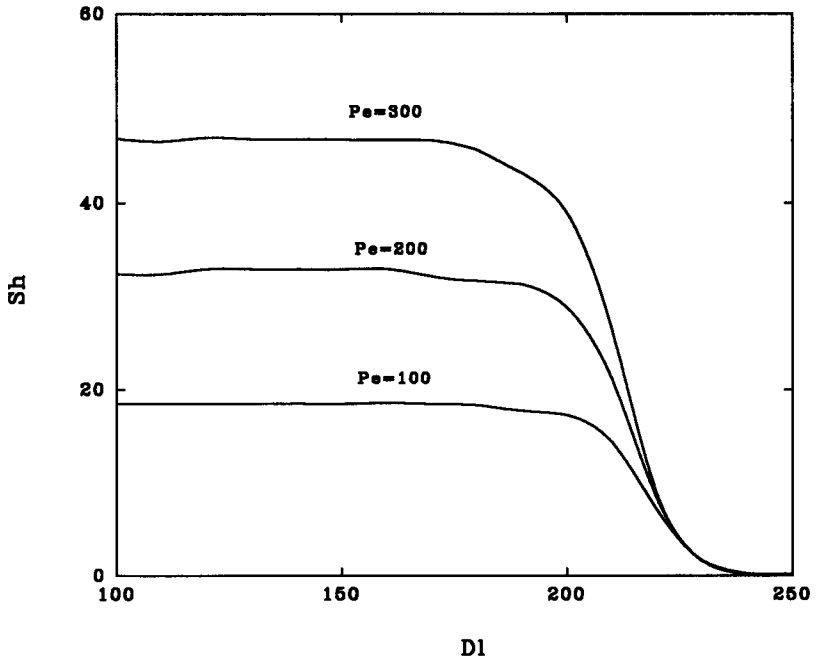

FIGURE 5 Dependence of Sh on Dl, calculated from Eqs. 4 and 5. $Ad = 0.02$, $\lambda/a = 0.4$, $\kappa a = 4212$, $Gr = 0.223$, and $\delta = 0.0001$.

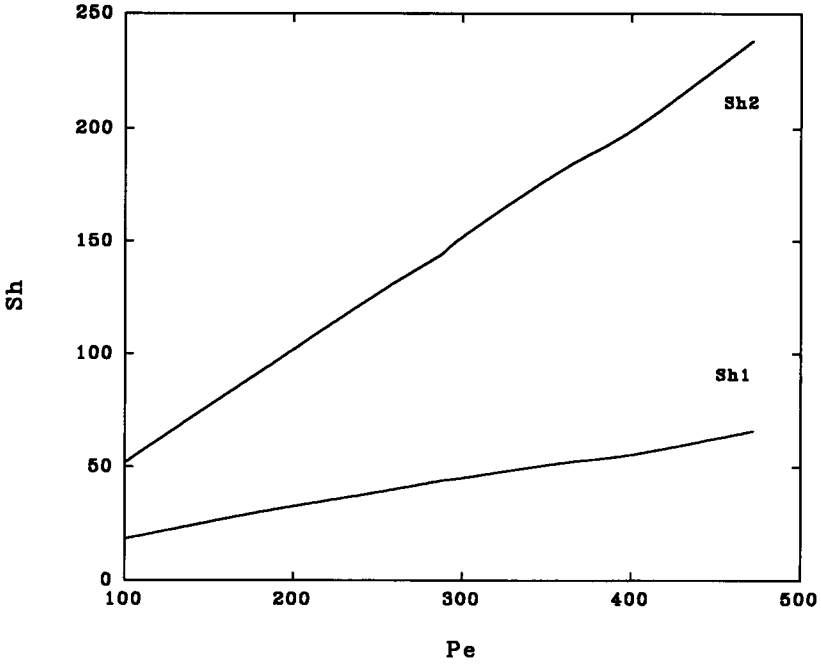

FIGURE 6 Calculated Sherwood number as a function of Peclet number, *Sh*1 and *Sh*2: numerical solution of Eqs. 4 and 5, with and without external forces and hydrodynamic interactions, respectively. $Ad = 0.2$, $Dl = 180$, $\lambda/a = 0.4$, $\kappa a = 4212$, and $Gr = 0.223$.

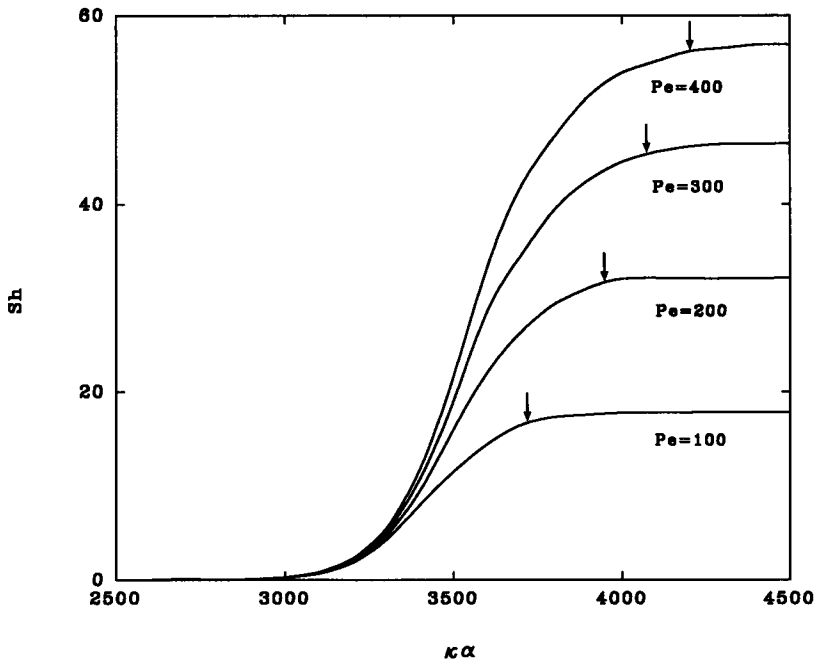

FIGURE 7 Sherwood number as a function of κa for four different *Pe* numbers. $Ad = 0.02$, $\lambda/a = 0.4$, $Gr = 0.223$, $Dl = 180$, and $\delta = 0.0001$. Arrows indicate CDC.

The effect of salt concentration on *Sh* is shown in Fig. 9. Theory predicts that no adhesion occurs at <50 mM NaCl, while exprimentally adhesions is observed at 10 mM NaCl. The dimensionless flux increases gradually with κa and reaches a plateau value at a salt concentration between 120 and 150 mM. Studies of the adhesion of fixed red blood cells to several hydrophobic polymer surfaces (Absolom et al., 1980) in the absence of flow have shown a similar trend. These investigators observed small amounts of adherent red cells at NaCl concentrations as low as 1 mM; plateau values were reached at around 100 mM NaCl, depending on the type of polymer. Similar results have been obtained with trypsin-treated red blood cells which begin to adhere on glass at 1 mM in the absence of flow (Trommler et al., 1985). The slow deposition rate (below the CDC) was found to be larger than predicted. Discrepancies between theoretical and experimental results for slow deposition or coagulation are common and not well understood. Nevertheless, the theoretical CDC is between 120 - 150 mM for $Dl = 180$, which is consistent with the experimental results. This CDC value is close to the physiological salt concentration and corresponds to a double layer thickness of 0.8–0.9 nm. At this *Dl* value, the product of the ζ potentials of the cell membrane and the glass surface is only 12 $(mV)^2$. If the ζ potential of −15 mV for red blood

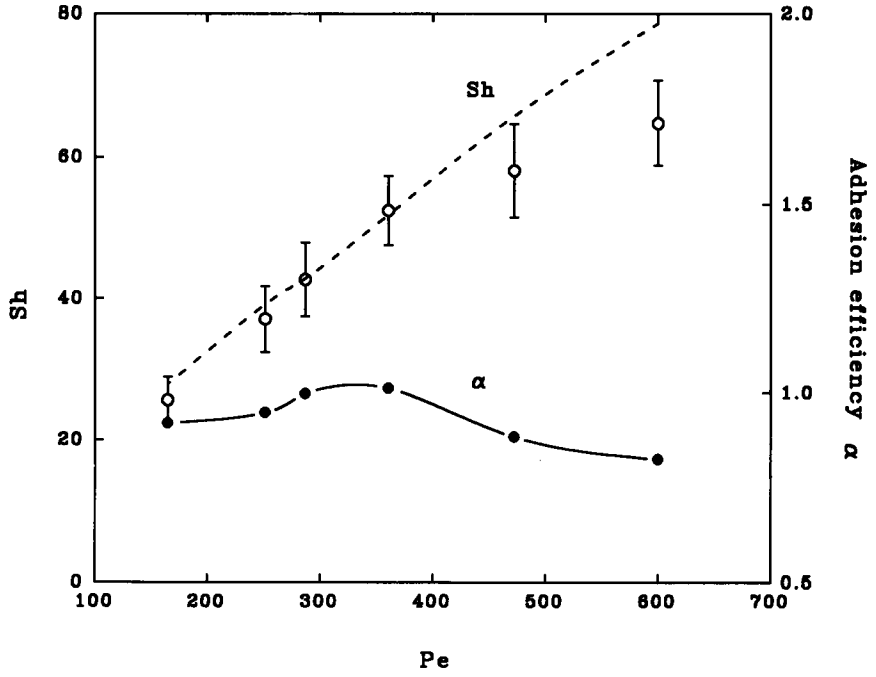

FIGURE 8 Experimental Sherwood number and adhesion efficiency as a function of Peclet number. The dashed line represents the theoretical prediction, $Sh1$.

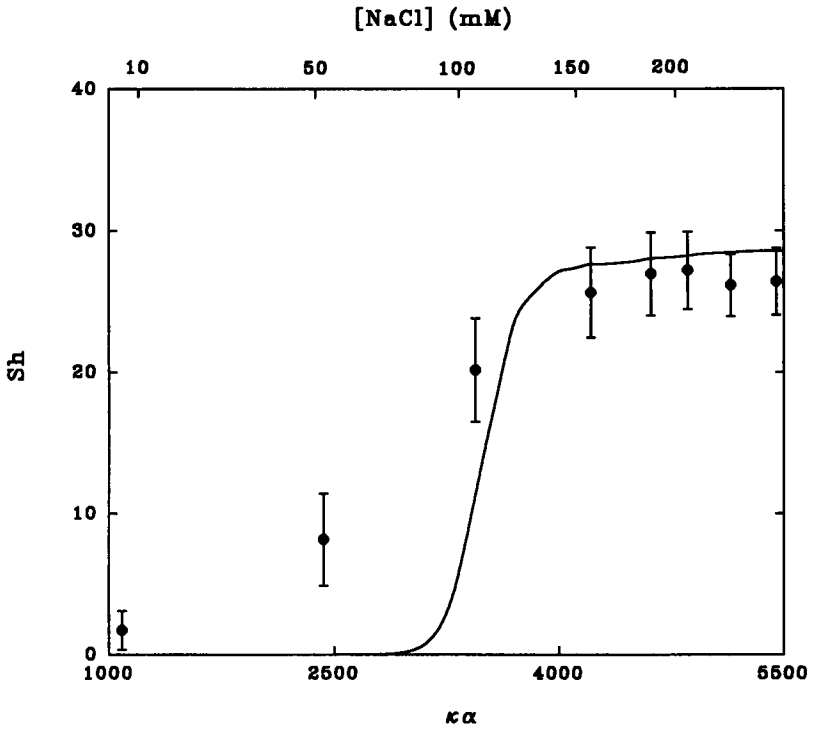

FIGURE 9 Experimental (*closed circles*) and theoretical values (*solid line*) of Sherwood number, *Sh*, as a function of κa at $Pe = 165$ and $Dl = 180$.

cells (see above) is correct, the ζ potential for glass at 0.15 M NaCl is only −0.8 mV.

Specific adhesion

The adhesion flux of type B red cells to anti-blood group B IgM-coated glass was also compared with the theory (Fig. 10). Specific adhesion occurs in a very narrow range of flow rates, typically 25–60 μl/s. Below this region, no adhesion was observed, presumably due to the steric repulsion between the albumin layer on the glass and the glycocalyx on the cells. Beyond this range, both specific and nonspecific adhesion were observed, as indicated by the nonzero surface flux of control (type A) cells. Despite the high affinity between an antigen and an antibody, the adhesion efficiency is less than 0.8 for all the flow rates used, a seemingly paradoxical result, if compared with the values obtained for nonspecific adhesion. However, only 0.26% of the surface area

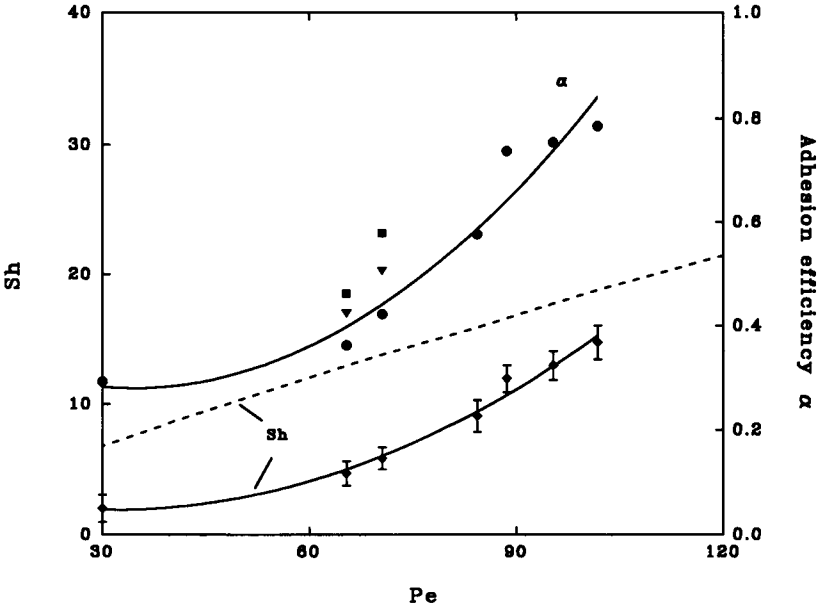

FIGURE 10 Dimensionless surface flux and adhesion efficiency for specific adhesion. Symbols: ◆, experimental *Sh* for antibody density 6 pmol/m^2; ●, efficiency for antibody density 6 pmol/m^2; ▼, efficiency for antibody density 7.3 pmol/m^2; ■, efficiency for antibody density 8.8 pmol/m^2. Dashed line represents the calculated values of *Sh*.

on glass is covered with antibody. This corresponds to an IgM density of 6 pmol m^{-2} for the 0.158 nmol liter^{-1} IgM used, and to about 104 antibody molecules per red cell projected area. Due to the curvature of the FSRC, the radius of the actual area where bridging is possible is much smaller. Assuming that the minimum separation distance, h_s, between the cell of radius a and the surface corresponds to the diameter of an albumin molecule (10 nm), and the maximum length for an antigen-antibody cross-bridge, h_b, corresponds to the diameter of an IgM molecule (30 nm), the radius of the cell/surface contact area can be estimated as $[a^2 - (a - h_b - h_s)^2]^{1/2} \simeq 0.35$ μm (Cozens-Roberts et al., 1990; Tha et al., 1986). Therefore, on average, there should be 1.4 antibody molecules in a "contact area" of 0.4 μm^2. Since the cells are rotating, while traveling along the surface, the area a cell covers in a complete rotation is $2\pi a l_w$, where $l_w = 0.7$ μm is the width of the area. The number of antigen-antibody bonds formed in this area (i.e., during the time of one cell rotation) can be expressed as

$$p = \beta f N_{ag} N_{ab} \tag{11}$$

where $N_{ag} = 2\pi a l_w N^*/4\pi a^2$ is the total number of antigen molecules in the area, N^* being the number of antigens on each red cell; $N_{ab} = 2\pi a l_w \sigma/\pi b_a^2$ is the total number of antibody molecules in the area, σ being the surface coverage of the antibody molecules of radius b_a. The probability, f, for an active site on an antibody to encounter an active site on an antigen can be estimated as $f = N_s(b_1/b_a)^2(b_2/d_a)^2$, where b_1 and b_2 are the radii of the active sites on an antibody and on an antigen, respectively, d_a is the radius of an antigen, and N_s is the number of the available variable regions on each IgM molecule on the surface. β in Eq. 11 is the efficiency of forming a bond. This efficiency of bond formation reflects the normal distance between an antigen and an antibody, as well as any effects of the potential energy of receptor/ligand interactions. Thus, Eq. 11 can be rewritten as

$$p = \beta \frac{b_1^2 b_2^2 l_w^2}{b_a^4 d_a^2} N^* N_s \sigma \tag{12}$$

Assuming that (i) the radius of the active sites of both the antigen and the antibody is 2 Å, (ii) the radius of the antigen is 5 nm, (iii) $N^* = 1 \times 10^6$ (Schenkel-Brunmer, 1980), and (iv) $N_s = 5$, p is found to be 8β, suggesting that, on average, a cell has to rotate only 45° to form a bond, provided it is sufficiently close to the surface. This high probability of bond formation is consistent with the high efficiency of specific adhesion at very low surface antibody coverage.

As indicated by the circles in Fig. 10, the adhesion efficiency is also affected by the flow rate. This can perhaps be explained by the dependence of the bond forming efficiency, β, on the antigen-antibody distance. The cells are closer to the surface when moving at a higher *Pe*, resulting in better contact with the antibody molecules. The data indicated by the triangles and squares in Fig. 10 confirm the fact that increasing the coating density improves the adhesion efficiency.

Fig. 11 shows the effect of cell shape and deformability on the adhesion rate. Fixed spherical cells show a higher adhesion efficiency than the fixed biconcave ones, even though the theoretical values have been corrected for the smaller hydrodynamic diameter (5.7 μm by PCS measurements) of the biconcave cells. This could be due to the fact that the membrane area of a biconcave cell which can participate in membrane/substrate contact is smaller than that of a spherical cell. Consequently, the probability of forming an antigen-antibody association is also smaller. Moreover, when a biconcave cell rotates along the surface, the average distance between the cell center and the substrate (~4 μm) tends to be larger than that for a spherical particle (~3 μ), which results in a lower adhesion rate.

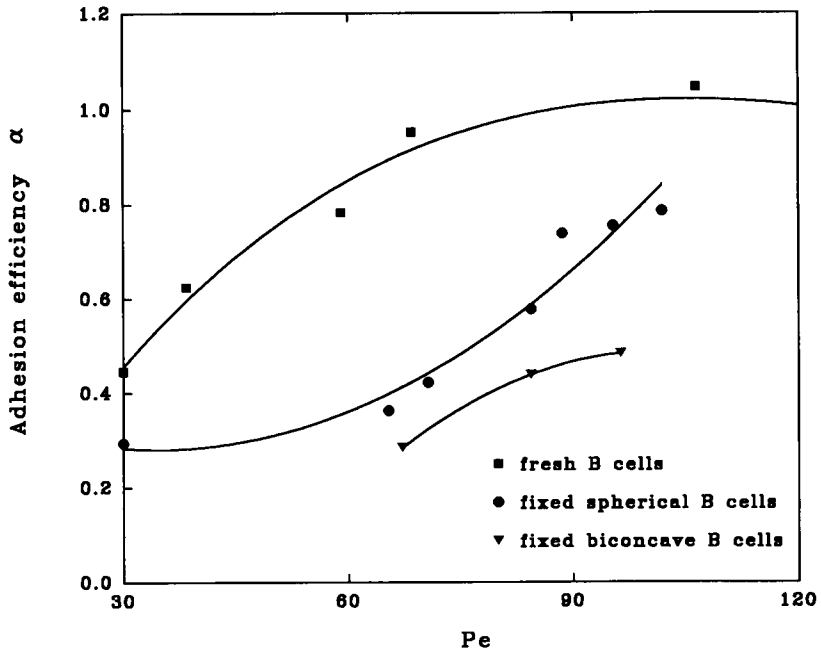

FIGURE 11 Effect of cell shape and rigidity. Symbols represent adhesion efficiencies for normal red cell suspensions (■); fixed spherical red cells (in sucrose/saline) (●); and fixed biconcave red cells (in sucrose/saline) (▼). Lines are a polynomial fit.

As regards the normal red cells, it should be noted that they were suspended in a saline solution (0.15 M NaCl), while the fixed cells were in a sucrose/saline solution. Despite the higher gravity force in saline, the normal cells adhered faster than fixed cells (spherical and biconcave). There are three possible explanations for this. First, although we have no direct evidence that fixation alters or destroys antigenic molecules, it does limit their mobility. Unfixed cells facilitate the adhesion by the migration of antigen to the initial contact area, thus reinforcing the bond strength, although this is unlikely to happen on a time scale of a collision. Second, the fixed cells are lacking in flexibility. The high rigidity prevents the cells from deforming, which otherwise would increase the secondary binding area around the initial contact area. This is consistent with the evidence that fixed red cells form large aggregates less readily than normal cells when exposed to antisera (Marquardt et al., 1984). Finally, antibody may be more effective in saline than in the presence of sucrose.

CONCLUDING REMARKS

The flow dependence of the surface flux of glutaraldehyde-fixed spherical swollen red blood cells to glass in a physiological salt solution containing 17% sucrose can be very well described by the numerical solution of the mass transport equation, taking into account hydrodynamic interactions as well as van der Waals attraction, electrostatic repulsion, and external gravity forces, and assuming that the product of the ζ potentials of the cell membrane and the glass is about 12 $(mV)^2$. The ratio of the experimental Sherwood number to the theoretical one, denoted as adhesion efficiency, is nearly unity at flow rates lower than 85 μl/s, while the adhesion efficiency drops at higher flow rates, due the increase in tangential force. For particles as large as erythrocytes, hydrodynamic interactions are not negligible, especially at high *Pe* numbers. The critical deposition concentration is found to occur at 120–150 mM NaCl, which is consistent with the theoretically predicted values. At low salt concentrations, the experimental values are larger than the theoretical ones. Creating steric repulsion by adsorbing a layer of albumin molecules on the glass completely prevents nonspecific adhesion at flow rates below 60 μl/s. Preincubating the glass with monoclonal IgM specific to blood group B antigen prior to albumin coating results in antigen-antibody mediated adhesion of type B cells but not of type A cells below that flow rate. At higher flow rates, both specific and nonspecific adhesion occur. The adhesion efficiency of this specific adhesion is a function of the concentration of the antibody on the surface and the flow rate. Despite the fact that only 0.3% of the surface was coated with antibody, the adhesion efficiency was about 80%. This is due to the large probability that an active antigen site will encounter an active antibody site during a single cell rotation. Cell shape and flexibility are also parameters that affect the adhesion rate. Compared to fixed biconcave red cells, fixed spherical cells have a larger adhesion efficiency. Normal red cells adhere more readily through antigen-antibody bonds than fixed cells, approaching 100% efficiency at large flow rates.

REFERENCES

Absolom, D. R., C. Thomson, G. Kruzyk, W. Zingg, and A. W. Neumann. 1986. Adhesion of hydrophilic particles (human erythrocytes) to polymer surfaces: effect of pH and ionic strength. *Colloids Surf.* 21:447–456.

Chien, S., S. Feng, M. Vayo, L. A. Sung, S. Usami, and R. Skalak. 1990. The dynamics of shear disaggregation of red blood cells in a flow channel. *Biorheology.* 27:135–147.

Cozens-Roberts, C., J. A. Quinn, and D. A. Lauffenburger. 1990. Receptor-mediated adhesion phenomena: model studies with the radial flow detachment assay. *Biophys. J.* 58:107–125.

Crunze, M., and C. C. Heuck. 1986. The surface charge of human

glutaraldehyde-fixed erythrocytes. *Biochim. Biophys. Acta.* 856:41–44.

Dabros, T., and T. G. M. van de Ven. 1983. A direct method for studying particle deposition onto solid surfaces. *Colloid & Polym. Sci.* 261:694–707.

Dintenfass, L. 1990. Blood as a near-"ideal" emulsion: a retrospective on the concept of the red cell as a fluid drop, its implications for the structure of the red cell membrane. *Biorheology.* 27:146–161.

Donath, E., and A. Voigt. 1986. Electrophoretic mobility of human erythrocytes. *Biophys. J.* 49:493–499.

Evans, E. A. 1983. Bending elastic modulus of red blood cell membrane derived from buckling instability of micropipet aspiration test. *Biophys. J.* 43:27–30.

Evans, E., and B. Kukan. 1983. Passive material behavior of granulocytes based on large deformation and recovery after deformation test. *Blood.* 64:1028–1035.

Feinstein, A., and E. A. Munn. 1969. Conformation of the free and antigen bound IgM antibody molecules. *Nature.* 224:1307–1309.

Fowler, H. W., and A. J. Mckay. 1980. The measurement of microbial adhesion. *In* Microbial Adhesion to Surfaces. R. C. W. Berkeley, J. M. Lynch, J. Melling, P. R. Rutter, and B. Vincent, editors. Ellis Horwood Ltd., Chichester, England. 143–159.

Gingell, D., and I. Todd. 1975. Adhesion of red blood cells to charged interfaces between immiscible liquids. A new method. *J. Cell Sci.* 18: 227–239.

Goldsmith, H. L., and J. Marlow. 1979. Flow behavior of erythrocytes. I. Rotation and deformation in dilute suspensions. *Proc. Roy. Soc. Lond. B* 182:351–384.

Gregory, J. 1969. The calculation of Hamaker constants. *Adv. Colloid Interface Sci.* 2:396–417.

Hull, M., and J. A. Kitchener. 1969. Interaction of spherical colloidal particles with planar surfaces. *Trans. Faraday Soc.* 65:3093–3104.

Hunter. R. J. 1987. *Foundations of Colloid Science.* Vol. 1. Oxford University Press Ltd., North Ireland. p. 673.

Kallay, N., and E. Matijevic. 1981. Particle adhesion and removal in model systems. IV. Kinetics of detachment of hematite particles from steel. *J. Colloid Interface Sci.* 83:289–300.

Levine, S., M. Levine, K. A. Sharp, and D. E. Brooks. 1983. Theory of the electrokinetic behavior of human erythrocytes. *Biophys. J.* 42:127–135.

Marquardt, D. L., L. J. Walker, and S. I. Wasserman. 1984. Adenosine receptors on mouse bone marrow-derived mast cells: functional significance and regulation by aminophylline. *J. Immunol.* 133:932–937.

Nir, S., and M. Anderson. 1976. van der Waals interactions between cell surfaces. *J. Membr. Biol.* 31:1–18.

Overbeek, J. T. G. 1952. Electrokinetic phenomena. *In* Colloid Science, H. R. Kruyt, editor. Elsevier Publishing Company, Amsterdam, The Netherlands. 194–243.

Parsegian, V. A., and D. Gingell. 1980. Red blood cell adhesion. III. Analysis of forces. *J. Cell Sci.* 41:151–157.

Rutter, P. R., and A. Abbott. 1978. A study of the interaction between oral streptococci and hard surfaces. *J. Gen. Microbiol.* 105:219–226.

Schenkel-Brunmer, H. 1980. Blood-group-ABH antigens of human erythrocytes. Quantitative studies on the distribution of H antigen sites among different classes of membrane components. *Eur. J. Biochem.* 104:529–534.

Shiga, T., M. Sekiya, N. Maeda, and S. Oka. 1985. Statistical determination of red cell adhesion to material surface by varying shear force. *J. Colloid Interface Sci.* 107:194–198.

Tha, S. P., J. Shuster, and H. L. Goldsmith. 1986. Interaction forces between red cells agglutinated by antibody. II. Measurement of hydrodynamic forces of breakup. *Biophys. J.* 50:1117–1126.

Trommler, A., D. Gingell, and H. Wolf. 1985. Red blood cells experience electrostatic repulsion but make molecular adhesions with glass. *Biophys. J.* 48:835–841.

Oss, C. J. 1975. The influence of the size and shape of molecules and particles on their electrophoretic mobility. *Sep. Purif. Methods.* 4:167–188.

Oss, C. J., and D. R. Absolom. 1983. Zeta potentials, van der Waals forces and hemagglutination. *Vox Sang.* 44:183–190.

Varennes, S., and T. G. M. van de Ven. 1988a. Effects of polyelectrolyte on the deposition and detachment of colloidal particles subjected to flow. *Colloids Surf.* 33:63–74.

Varennes, S., and T. G. M. van de Ven. 1988b. Effects of polymers on the detachment of polymer coated latex particles from glass surfaces. *PhysicoChem. Hydrodyn.* 10:415–428.

Vertessy, B. G., and T. L. Steck. 1989. Elasticity of the human red cell membrane skeleton. Effects of temperature and denaturants. *Biophys. J.* 55:255–262.

Visser, J. 1972. On Hamaker constants: a comparison between Hamaker consants and Lifshitz-van der Waals constants. *Adv. Colloid Interface Sci.* 3:331–363.

Volger, E. A., and R. W. Bussian. 1987. Short-term cell-attachment rates: a surface-sensitive test of cell-substrate. *J. Biomed. Mates. Res.* 21:1197–1211.

Weiss, L. 1974. Studies of cellular adhesion in tissue culture. XIV. Positively charged surface groups and the rate of cell adhesion. *Exp. Cell Res.* 83: 311–318.

Wolf, H., and D. Gingell. 1983. Conformational response of the glycocalyx to ionic strength and interaction with modified glass surfaces: study of live red cells by interferometry. *J. Cell Sci.* 63:101–112.

Xia, Z., L. Woo, and T. G. M. van de Ven. 1989. Microrheological aspects of adhesion of *Eschrichia coli* on glass. *Biorheology.* 26:359–375.